ASTEROIDS

Dating the Solar System's giant planet orbital instability using enstatite meteorites

Chrysa Avdellidou[1,2]*, Marco Delbo'[1,2], David Nesvorný[3], Kevin J. Walsh[3], Alessandro Morbidelli[1,4]

The giant planets of the Solar System formed on initially compact orbits, which transitioned to the current wider configuration by means of an orbital instability. The timing of that instability is poorly constrained. In this work, we use dynamical simulations to demonstrate that the instability implanted planetesimal fragments from the terrestrial planet region into the asteroid main belt. We use meteorite data to show that the implantation occurred >60 million years (Myr) after the Solar System began to form. Combining this constraint with a previous upper limit derived from Jupiter's trojan asteroids, we conclude that the orbital instability occurred 60 to 100 Myr after the beginning of Solar System formation. The giant impact that formed the Moon occurred within this range, so it might be related to the giant planet instability.

If a meteorite type can be linked to a specific parent asteroid, it provides insight into the asteroid's composition, time of formation, temperature evolution, and original size. During the cooling process of a parent asteroid, it reaches the closure temperatures of different isotopic systems at successive epochs, which are recorded in meteorites derived from that asteroid. The isotopic abundance ratio of each system varies with known radioactive decay constants. Measurements of the isotopic abundances can determine the epoch at which each system closed, called thermochronometry, which constructs cooling curves of temperature as a function of time. Therefore, thermochronometers in meteorites can constrain the epoch at which major collisional events disturbed the cooling curves of the parent asteroid (*1*).

The group of meteorites classified as low-iron enstatite chondrites (ELs) have been linked to the Athor family of asteroid fragments, whose largest member is (161) Athor (*2*). Spectroscopy and albedo measurements of the Athor family match the properties of ELs, and their orbits in the asteroid main belt are dynamically favorable for the transfer of fragments to Earth, where they fall as meteorites (*2*). The Athor family was produced by an asteroid collision ~3 billion years ago, which catastrophically destroyed a progenitor asteroid (*2*). The estimated size of the Athor family progenitor is 64 km, derived from the known family members and taking into account the dynamical and collisional loss of family members that has occurred since the collision (*2*). However, thermochronometry of ELs (*1*) requires the primordial parent body of the ELs (hereafter referred to as the EL planetesimal) to have had a diameter of 240 to 420 km. The EL planetesimal was therefore much bigger than the Athor family progenitor (*2*). This size mismatch can be resolved if the Athor family progenitor was itself a collisional fragment of the EL planetesimal (*2*).

The collision that fragmented the EL planetesimal could not have happened in the asteroid belt; otherwise, it would have produced a much larger family of fragments in the main belt than the Athor family, which has been excluded by observations (*2*, *3*). This is consistent with meteoritic evidence that the EL planetesimal formed in the terrestrial planet region [orbital semimajor axis $a \sim 1$ astronomical unit (au); Fig. 1], as indicated by the isotopic similarity of ELs with Earth and their similar low rock oxidation (*4*, *5*).

We propose that after the breakup of the EL planetesimal, the Athor family progenitor (and possibly other fragments or other planetesimals from the terrestrial planet region) was implanted into the main belt by some dynamical process. After its capture in the main belt, the Athor family progenitor was disrupted by another collision, which generated the currently observed family (Fig. 1). We test this scenario by investigating both how fragments of the EL planetesimal could be implanted into the region where the Athor family progenitor was disrupted and when the implantation could have taken place.

Dating the EL planetesimal breakup

Meteorite evidence has shown that the EL planetesimal accreted 1.8 to 2.1 million years (Myr) after the beginning of Solar System formation (*1*), where the latter is defined by the formation of calcium-aluminum–rich inclusions (CAIs) (*6*). The EL planetesimal was initially heated by the decay of radioactive elements and then cooled for several tens of millions of years, as indicated by thermochronometers (*1*). The EL planetesimal must have broken up after this phase.

To establish a lower limit on the epoch of the breakup, we modeled (*7*) the cooling of the material that later became the ELs using two possible scenarios for the formation of the Athor family progenitor (fig. S1). In the first scenario, the Athor family progenitor was a large fragment consisting of a single rock (monolithic), which would cool slowly after the impact. In the second scenario, the Athor family progenitor formed by the reaccumulation of numerous small fragments (*8*, *9*), which would have cooled almost instantaneously. We find that both scenarios can be consistent with the meteorite thermochronometer data, but the probability of being consistent decreases with a decreasing breakup epoch, which means that it becomes less likely at earlier times (fig. S1). We exclude a breakup of the EL planetesimal before 57 and 59 Myr for the first and second scenarios, respectively, at 95% confidence (*7*). We therefore adopt a lower limit on the timing of the EL planetesimal breakup of >60 Myr after Solar System formation.

Implantation after terrestrial planet formation

We investigate several possible scenarios for implanting fragments of the EL planetesimal into the main belt. Initially, we assume that by 60 Myr after Solar System formation, all planets had fully formed and reached their current orbits. For this first scenario, we simulated 10,000 particles in the terrestrial planet region ($0.6 < a < 1.6$ au), representing planetesimals or fragments thereof, and dynamically evolved their orbits for 50 Myr. We found that encounters with terrestrial planets changed the orbital semimajor axes of these particles, producing a scattered disk of objects, which we refer to as the terrestrial scattered disk (Fig. 2A). In our simulation (fig. S2), after the first 20 Myr of evolution, an average of 1.7 ± 0.4% (*7*) of the surviving planetesimals have orbits with semimajor axes in the inner main belt range ($2.0 < a < 2.5$ au) but with a larger eccentricity ($e \gtrsim 0.2$) than that of the main belt. Some temporary captures of objects into the main belt happen at specific semimajor axes that are resonant with the orbital frequency of planets, but none of these particles reach the region of Athor's orbit (we do not extend it until 2.5 au to avoid the 3:1 mean motion resonance with Jupiter, which has a considerable width) (Fig. 2A). All such resonant orbits are located far from Athor's orbit (*10*). We conclude that implantation of the EL planetesimal to Athor's orbit is not possible if the planets are on their current orbits, so we exclude this scenario.

Implantation during terrestrial planet formation

Resolving this problem requires some process that is not operating in the current Solar

[1]Laboratoire Lagrange, Centre National de la Recherche Scientifique, Observatoire de la Côte d'Azur, Université Côte d'Azur, 06304 Nice, France. [2]School of Physics and Astronomy, University of Leicester, Leicester LE1 7RH, UK. [3]Southwest Research Institute, Boulder, CO 80302, USA. [4]Collège de France, Centre National de la Recherche Scientifique, Université Paris Sciences et Lettres, Sorbonne Université, 75014 Paris, France.
*Corresponding author. Email: c.avdellidou@leicester.ac.uk

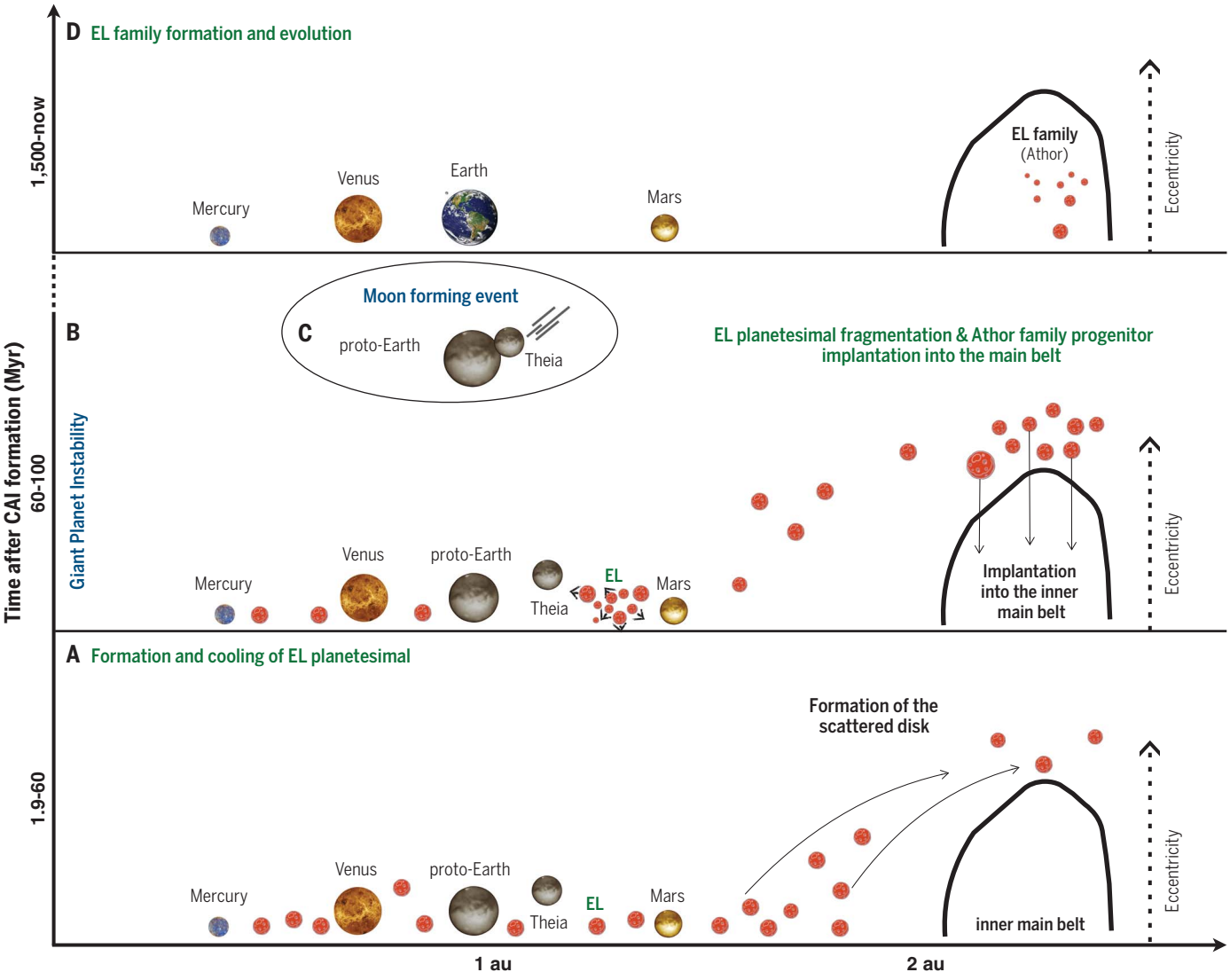

Fig. 1. Schematic diagram of our preferred scenario. Red circles are planetesimals (and their fragments) from the terrestrial planet region. The black solid curves roughly denote the boundary of the current asteroid inner main belt. Eccentricity increases from bottom to top. Each panel shows the proposed evolution of the inner Solar System at different time ranges: (**A**) Formation and cooling of the EL planetesimal in the terrestrial planet region before 60 Myr after Solar System formation. In this period, the terrestrial planets began scattering planetesimals to orbits with high eccentricity and semimajor axes that correspond to the asteroid main belt. (**B**) Between 60 and 100 Myr, the EL planetesimal was destroyed by an impact in the terrestrial planet region. At least one fragment (the Athor family progenitor) was scattered by the terrestrial planets into the scattered disk, as in (A), then the giant planet instability implanted it into the inner main belt by decreasing its eccentricity. (**C**) A few tens of millions of years after the giant planet instability occurred, a giant impact between the planetary embryo Theia and proto-Earth formed the Moon. (**D**) The Athor family progenitor experienced another impact event that formed the Athor family at ~1500 Myr.

System, can permanently reduce orbital eccentricities, and operates at locations different from those of the current orbital resonances. As a second scenario, we investigated whether this could occur during the time of terrestrial planet formation.

Implantation of planetesimals from the terrestrial planet region into the main belt has been previously reported (*11*, *12*). To quantify the implantation probability as a function of time, we selected only simulations of the formation of the planets that reproduce the final masses and orbits of the terrestrial planets. We adopted a previous simulation [simulation 35 in (*13*)] that produced planets almost identical to the current Solar System. In that simulation, the planet accretion process was fed by a combination of planetary embryos and 44,000 planetesimals, where embryos were assumed to have been accreted from planetesimals and pebbles. All of these bodies had initial $a < 1.5$ au at the time of the dispersal of the gas of the protoplanetary disk, which happened 4 to 5 Myr after the formation of CAIs (*14*). The removal of the gas from the protoplanetary disk allows planetesimal scattering at large distances; this was not possible at earlier times because of gas drag. Following the planetesimal evolution up to 200 Myr, we found that after 60 Myr, only one object—which started at $a = 1.167$ au—entered the region of Athor's orbit (at ~100 Myr) as a result of a resonance with Mars. However, this object had an unstable orbit and exited the main belt after another 1 Myr. We calculated the probability of planetesimal implantation in the region of Athor's orbit after 60 Myr as $<2 \times 10^{-5}$ in this simulation. We therefore exclude the second scenario as well.

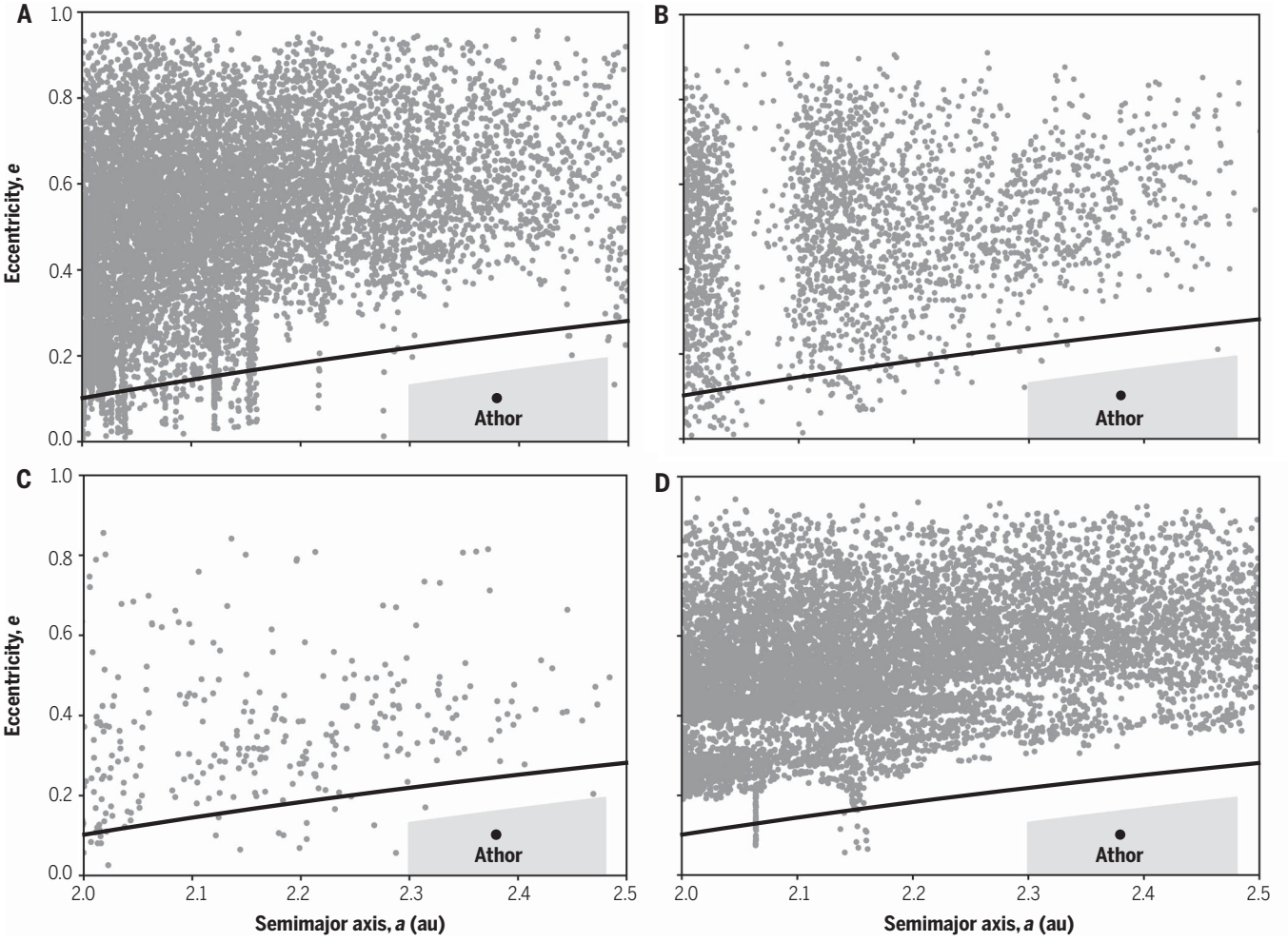

Fig. 2. Simulated terrestrial scattered disk. In all panels, gray circles are individual particles in our simulations. The displayed semimajor axis range 2.0 < a < 2.5 au corresponds to the inner main belt. The black line is the eccentricity limit of the inner main belt, approximated as e = 1 to 1.8/a. Objects above the line cross the orbit of Mars and so are unstable. The black dot is the current orbit of the asteroid (161) Athor, and the gray shaded area around it has 2.3 < a < 2.48, e > 1 to 2.0/a, and i < 15°, which is our definition of the region around it (as discussed in the text). Each panel is a snapshot from the simulations showing the inner main belt architecture: (**A**) With terrestrial and giant planets on their current orbits after 20 Myr. (**B**) With no terrestrial planets and only Theia on an eccentric orbit crossing the main belt after 10 Myr. (**C**) With all planets on their current orbits and Theia on the same orbit as in (B) after 10 Myr. (**D**) With the giant planets on their preinstability orbits after 35 Myr. In all cases, particles are implanted into the main belt but none in the region around Athor's orbit.

The role of Theia

Earth's Moon is thought to have formed by a giant impact with a planetary embryo known as Theia. In the same simulation [simulation 35 in (*13*)], terrestrial planet formation ends with the last giant impact, 41.2 Myr after gas dispersal. This terrestrial planet formation timescale is typical of simulations that assume that the giant planets were on, or quickly evolved to, their current orbits (*15*). Although it does not typically occur in the simulations, it is possible that in the real Solar System, one embryo (Theia) remained after this time before colliding with Earth. To investigate this evolution, we ran two simulations for 10 Myr, each containing 10,000 particles generated by cloning the terrestrial scattered disk objects with 2.0 < a < 2.5 au from the first scenario (Fig. 2A). For this third scenario, we assumed a Mars-mass Theia on an orbit much more eccentric (e > 0.40) than is typically considered (*16*), which enhances planetesimal implantation because of Theia repeatedly crossing the inner asteroid belt.

In the first simulation, for simplicity, we removed all the terrestrial planets except Theia, so its orbit is stable rather than evolving in an uncontrolled manner. We found that a few planetesimals are implanted in the inner main belt (Fig. 2B). However, the probability of implanting in the region of Athor's orbit is $<10^{-6}$ (no object was captured). In the second simulation, we included the terrestrial planets as well as Theia; Earth was assumed to have 90% of its current mass, and all terrestrial planets were initially on their current orbits. The original orbit of Theia was as before but now evolved chaotically because of encounters with the terrestrial planets. To sample possible evolutions of Theia, we performed 10 simulations with 1000 particles each. Theia's evolution is different in each of these simulations. Combining the results, we found that the number of particles implanted in the inner asteroid belt is substantially smaller than in the previous case (Theia alone); again, no particles were implanted in the region of Athor's orbit (Fig. 2C). Implantation might be possible if the simulation assumed a higher Theia mass, but that would produce a giant impact that is inconsistent with the Moon-forming impact (*16*, *17*). We therefore also exclude this third scenario.

Implantation during the giant planet instability

A fourth scenario is that at the time of the breakup of the EL planetesimal, the giant planets were not yet on their current orbits.

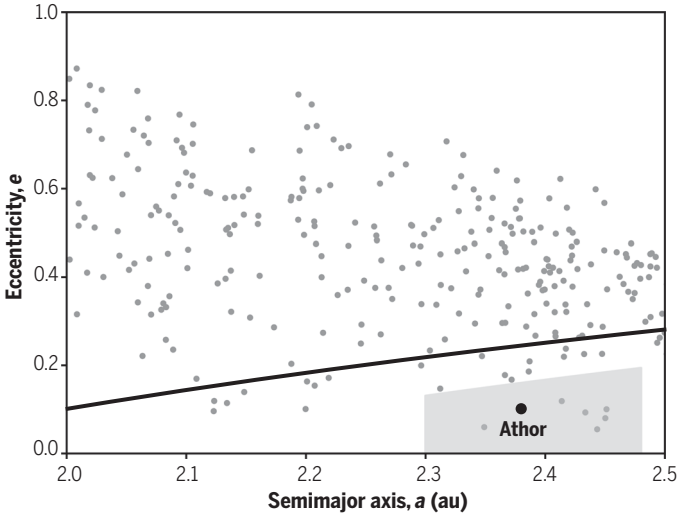

Fig. 3. Simulated terrestrial scattered disk after the giant planet instability. Same as Fig. 2, but for a simulation in which the giant planet instability has occurred. From 10,000 particles in the simulation, 28 have reached the main belt and 6 of those are in the region around Athor's orbit.

Previous work has shown that when gas was removed from the protoplanetary disk, the giant planets had orbits in a resonant chain, so each planet was in resonance with its neighbors (*18*). The orbits were more circular and coplanar, and the system had a more compact configuration than it does today. The current orbits of the giant planets were acquired during a phase of temporary orbital instability (*19*) triggered by the planets' interactions with a massive disk of trans-neptunian planetesimals (*20*) or with the dissipating disk of gas (*21*). Implantation of EL planetesimal fragments into the main belt could then occur during the giant planet instability. However, it is not well known when that instability occurred. It has been proposed to have occurred ~600 Myr after the formation of CAIs, during a putative late heavy bombardment of small bodies on the Moon (*22*). However, the instability is likely to have occurred much earlier, and the existence of the late heavy bombardment is doubtful (*23*–*25*). The preservation of binary objects in the trans-neptunian region indicates that the instability occurred within the first 100 Myr after the formation of CAIs (*26*).

We studied the effect of the giant planet instability on the terrestrial scattered disk of planetesimals and the probability of their implantation in the region of Athor's orbit. Previous simulations of the giant planet instability [case 1 in (*27*)] have strongly modified and dispersed the eccentricities and inclinations of objects with semimajor axes corresponding to the main belt (*28*), indicating that objects can be implanted from the terrestrial scatter disk into the main belt. To test this scenario, we do not reuse the terrestrial planet scattered disk from the above scenario, but rather resimulate it with the giant planets on a set of assumed preinstability orbits. As before, we simulated 10,000 particles initially in the terrestrial planet region. Because of the smaller orbital eccentricities of the giant planets, the terrestrial scattered disk was less perturbed, it was less dispersed than, and its particles took longer to impact the Sun, impact a planet, or be ejected from the Solar System compared with our earlier simulation. After ~35 Myr, an average of 5.3 ± 0.3% (*7*) of the surviving planetesimals had orbits with $2.0 < a < 2.5$ au (fig. S1) (higher than the 1.7% found above for the simulation with planets on their current orbits), although their perihelion distances were <1.8 au (Fig. 2D). The only temporary capture into the asteroid belt occurs at the location of the 3:1 mean motion resonance with Jupiter, which was at 2.6 au at the time. We cloned 10,000 particles from those terrestrial scattered disk objects with $2.0 < a < 2.5$ au and simulated the particles' orbital evolution during the giant planet instability [case 1 in (*27*)] for 10 Myr. In this case, we found several particles implanted in the inner main belt (Fig. 3). We calculated (*7*) average implantation probabilities P_I to be $(1.48 \pm 0.29) \times 10^{-4}$ in the inner main belt and $(3.18 \pm 1.30) \times 10^{-5}$ in the region of Athor's orbit. We also estimated 99.5% likelihood (3σ) lower limits of $P_I > 8.5 \times 10^{-5}$ and $P_I > 1 \times 10^{-5}$ in the inner main belt and in the region of Athor's orbit, respectively (*7*).

To evaluate whether this probability is large enough to explain the implantation of Athor, we estimated (*7*) the planetesimal population mass M_P, converted it to a number of objects N_P, and multiplied this by P_I to obtain the expected number of implanted objects N_I. We determined M_P by considering that accretion of planetesimals that collided with Earth after the Moon-forming event (known as the late veneer) (*25*) delivered $M_{LV} = (4.86 \pm 1.63) \times 10^{-3}$ Earth masses (*29*) of material. This is a fraction R of the total mass in planetesimals that were still present in the terrestrial planet region at the time of the Moon-forming event. Using previous investigations of the late veneer (*25*), we estimated $R = 0.12 \pm 0.04$ (*7*). To estimate N_P, we compared the total planetesimal mass $M_P = M_{LV}/R$ with the current mass of the main belt M_{MB}, which is 4×10^{-4} Earth masses (*30*). We estimated M_{MB} from measurements of 607 asteroids with diameters larger than 50 km (*31*) (data S1), which have a planetesimal-like size distribution and so are interpreted as leftover planetesimals (*32*, *33*). The 50-km diameter threshold was selected (in the previous work) to include leftover planetesimals but exclude contamination by families of fragments generated by collisions in the main belt (*32*). Therefore, the expected number of implanted planetesimals (or fragments thereof) is

$$N_I = P_I \times M_{LV}/R \times N_{ast}/M_{MB} \quad (1)$$

We find $N_I = 9 \pm 4$ and $N_I = 1.9 \pm 0.9$, on average, in the inner main belt and the region of Athor's orbit, respectively, where the uncertainties are 1σ (*7*, *34*). The corresponding 99.5% lower limits are $N_I > 5.2$ and $N_I > 0.6$, respectively. These estimates based on our simulations are consistent with astronomical observations, which have found (*35*) five leftover planetesimals in the inner main belt with spectra matching enstatite chondrites (*2*). One of those five—the only one in the region of Athor's orbit—is Athor itself. This calculation implicitly assumes that most of the planetesimals scattered from the terrestrial planet region had enstatite compositions, consistent with isotopic constraints on the composition of the late veneer (*5*, *36*). We conclude that the giant planet orbital instability is capable of implanting scattered planetesimals from the terrestrial planet region into Athor's current orbit.

Implications for the early Solar System

Because the implantation of the Athor family progenitor could not have occurred before the breakup of the original EL planetesimal (determined above as after 60 Myr), our results provide a lower limit on the timing of the giant planet instability of >60 Myr. A 95% upper limit of <100 Myr has previously been derived from the Patroclus-Menoetius binary asteroid—one of Jupiter's trojans (*26*). We conclude that the giant planet instability occurred between 60 Myr and 100 Myr (Fig. 1). This excludes the possibility of an earlier instability (*21*, *37*) occurring just after gas removal from the protoplanetary disk (*21*), which has been proposed to explain the mass of Mars (*37*) and was adopted in previous simulations (*13*).

The parent bodies of two groups of meteorites, classified as low-iron (L) and high-iron (H) ordinary chondrites, suffered catastrophic impacts ~60 Myr after the formation of CAIs (*38*), equaling our lower limit on the giant planet instability (supplementary text). The embedding of H and L chondritic fragments as foreign rocks (xenoliths) in nonchondritic ureilite-type meteorites probably occurred around the same time because it requires a large number

of fragments to have been present in the main belt (*39*). The close to simultaneous disruption of the H and L parent bodies indicates an increase in the orbital eccentricities and inclination of the asteroids in the main belt, which has been interpreted as being caused by the giant planet instability (*39*).

The formation of the Moon (*40*–*42*) also occurred within the range that we determined for the giant planet instability. This might be a coincidence, or there might be a causal relationship between the two events. Dynamical simulations have shown that a stable system of five terrestrial planets (Mercury, Venus, Earth, Mars, and Theia) can experience the Moon-forming impact within a few tens of millions of years after the giant planet instability (*16*, *43*). Such a five-planet system has a higher probability to form (and remain stable) if the giant planets are on almost circular orbits before the instability and if the initial planetesimals were concentrated near 1 au (*44*). We therefore suggest that the giant planet instability is not related to the late heavy bombardment of the Moon (*22*) but could instead be related to the formation of the Moon itself.

REFERENCES AND NOTES

1. M. Trieloff, J. Hopp, H.-P. Gail, *Icarus* **373**, 114762 (2022).
2. C. Avdellidou *et al*., *Astron. Astrophys.* **665**, L9 (2022).
3. M. Delbo, C. Avdellidou, A. Morbidelli, *Astron. Astrophys.* **624**, A69 (2019).
4. M. Javoy *et al*., *Earth Planet. Sci. Lett.* **293**, 259–268 (2010).
5. N. Dauphas, *Nature* **541**, 521–524 (2017).
6. Y. Amelin *et al*., *Earth Planet. Sci. Lett.* **300**, 343–350 (2010).
7. Materials and methods are available as supplementary materials.
8. P. Michel, W. Benz, P. Tanga, D. C. Richardson, *Science* **294**, 1696–1700 (2001).
9. D. Nesvorný, W. F. Bottke Jr., L. Dones, H. F. Levison, *Nature* **417**, 720–771 (2002).
10. A. Morbidelli, D. Nesvorný, *Icarus* **139**, 295–308 (1999).
11. W. F. Bottke, D. Nesvorný, R. E. Grimm, A. Morbidelli, D. P. O'Brien, *Nature* **439**, 821–824 (2006).
12. S. N. Raymond, A. Izidoro, *Sci. Adv.* **3**, e1701138 (2017).
13. D. Nesvorný, F. V. Roig, R. Deienno, *Astron. J.* **161**, 50 (2021).
14. B. P. Weiss, X.-N. Bai, R. R. Fu, *Sci. Adv.* **7**, eaba5967 (2021).
15. D. P. O'Brien, A. Morbidelli, H. F. Levison, *Icarus* **184**, 39–58 (2006).
16. S. R. DeSouza, F. Roig, D. Nesvorný, *Mon. Not. R. Astron. Soc.* **507**, 539–547 (2021).
17. R. M. Canup, *Science* **338**, 1052–1055 (2012).
18. A. Morbidelli, K. Tsiganis, A. Crida, H. F. Levison, R. Gomes, *Astron. J.* **134**, 1790–1798 (2007).
19. D. Nesvorný, A. Morbidelli, *Astron. J.* **144**, 117 (2012).
20. K. Tsiganis, R. Gomes, A. Morbidelli, H. F. Levison, *Nature* **435**, 459–461 (2005).
21. B. Liu, S. N. Raymond, S. A. Jacobson, *Nature* **604**, 643–646 (2022).
22. R. Gomes, H. F. Levison, K. Tsiganis, A. Morbidelli, *Nature* **435**, 466–469 (2005).
23. N. E. B. Zellner, *Orig. Life Evol. Biosph.* **47**, 261–280 (2017).
24. A. Morbidelli *et al*., *Icarus* **305**, 262–276 (2018).
25. D. Nesvorný *et al*., *Astrophys. J. Lett.* **941**, L9 (2022).
26. D. Nesvorný, D. Vokrouhlický, W. F. Bottke, H. F. Levison, *Nat. Astron.* **2**, 878–882 (2018).
27. D. Nesvorný, D. Vokrouhlický, A. Morbidelli, *Astrophys. J.* **768**, 45 (2013).
28. P. I. O. Brasil *et al*., *Icarus* **266**, 142–151 (2016).
29. R. J. Walker, *Geochemistry* **69**, 101–125 (2009).
30. E. V. Pitjeva, N. P. Pitjev, *Astron. Lett.* **44**, 554–566 (2018).
31. The Minor Planet Physical Properties Catalogue; https://mp3c.oca.eu/ [accessed 23 September 2023].
32. M. Delbo', K. Walsh, B. Bolin, C. Avdellidou, A. Morbidelli, *Science* **357**, 1026–1029 (2017).
33. B. Polak, H. Klahr, *Astrophys. J.* **943**, 125 (2023).
34. J. R. Taylor, *An Introduction to Error Analysis: The Study of Uncertainties in Physical Measurements* (University Science Books, ed. 2, 1996).
35. J. Bourdelle de Micas *et al*., *Astron. Astrophys.* **665**, A83 (2022).
36. M. Fischer-Gödde, T. Kleine, *Nature* **541**, 525–527 (2017).
37. M. S. Clement, N. A. Kaib, S. N. Raymond, K. J. Walsh, *Icarus* **311**, 340–356 (2018).
38. T. Blackburn, C. M. O. Alexander, R. Carlson, L. T. Elkins-Tanton, *Geochim. Cosmochim. Acta* **200**, 201–217 (2017).
39. C. A. Goodrich *et al*., *Planet. Sci. J.* **2**, 13 (2021).
40. S. A. Jacobson *et al*., *Nature* **508**, 84–87 (2014).
41. W. F. Bottke *et al*., *Science* **348**, 321–323 (2015).
42. M. Maurice, N. Tosi, S. Schwinger, D. Breuer, T. Kleine, *Sci. Adv.* **6**, eaba8949 (2020).
43. M. S. Clement, R. Deienno, A. Izidoro, *Icarus* **389**, 115260 (2023).
44. A. Izidoro, S. N. Raymond, A. Morbidelli, O. C. Winter, *Mon. Not. R. Astron. Soc.* **453**, 3619–3634 (2015).
45. C. Avdellidou, Replication Data for: Dating Solar System's giant planet orbital instability using enstatite meteorites, Harvard Dataverse (2024); https://doi.org/10.7910/DVN/KHO1ZY.

ACKNOWLEDGMENTS

We acknowledge use of data provided by the Minor Planet Physical Properties Catalogue (MP3C) of the Observatoire de la Côte d'Azur. **Funding:** C.A., M.D., and A.M. acknowledge support from the French National Research Agency (ANR-18-CE31-0014). D.N. acknowledges support from the NASA Solar System Workings program. K.J.W. acknowledges support from the NASA Solar System Exploration Research Virtual Institute node, cooperative agreement no. 80ARC0M0008. A.M. acknowledges support from the European Research Council advanced grant no. 101019380. **Author contributions:** A.M. performed the numerical simulations, and M.D. developed the thermal evolution model. A.M., C.A., M.D., and D.N. contributed formal analysis. C.A., A.M., M.D., and K.J.W. contributed to the conceptualization and writing. **Competing interests:** The authors declare no competing interests. **Data and materials availability:** The output of our thermal evolution calculations, output of our dynamical simulations, our scripts for converting the implantation probability to the number of bodies, and our plotting scripts are archived at Harvard Dataverse (*45*). The properties of current main belt asteroids are available in data S1, which was selected from MP3C (*31*).

SUPPLEMENTARY MATERIALS

science.org/doi/10.1126/science.adg8092
Materials and Methods
Supplementary Text
Figs. S1 and S2
References (*46*–*60*)
Data S1

Submitted 30 January 2023; accepted 16 February 2024
Published online 16 April 2024
10.1126/science.adg8092